Role of Hydrogen in Chemical Vapor Deposition Growth of Large Single-Crystal Graphene

Ivan Vlassiouk,[†,*] Murari Regmi,[‡] Pasquale Fulvio,[⊥] Sheng Dai,[⊥] Panos Datskos,[†] Gyula Eres,[‡] and Sergei Smirnov*[,§]

[†]Measurement Science & System Engineering Division, [‡]Materials Science and Technology Division, and [⊥]Chemical Sciences Division, Oak Ridge National Laboratory, Oak Ridge, Tennessee 37831, United States and [§]Department of Chemistry and Biochemistry, New Mexico State University, Las Cruces, New Mexico 88003, United States

ABSTRACT We show that graphene chemical vapor deposition growth on copper foil using methane as a carbon source is strongly affected by hydrogen, which appears to serve a dual role: an activator of the surface bound carbon that is necessary for monolayer growth and an etching reagent that controls the size and morphology of the graphene domains. The resulting growth rate for a fixed methane partial pressure has a maximum at hydrogen partial pressures 200—400 times that of methane. The morphology and size of the graphene domains, as well as the number of layers, change with hydrogen pressure from irregularly shaped incomplete bilayers to well-defined perfect single layer hexagons. Raman spectra suggest the zigzag termination in the hexagons as more stable than the armchair edges.

KEYWORDS: graphene · CVD · grain · domain · mechanism · hydrogen · hexagons

Graphene is a two-dimensional carbon material that has attracted great scientific and technological interest due to its intriguing physical properties and enormous potential for various applications.[1−3] Initially reported micromechanical exfoliation of highly oriented pyrolytic graphite (HOPG) provides minute amounts of high quality graphene. This method is labor intensive and difficult to reproduce. Moreover, large quantities of the graphene sheets of desired dimensions, required for most applications, cannot be obtained from this method. Recently, several high-throughput approaches for graphene synthesis such as chemical vapor deposition (CVD)[4] and reduction of graphene oxide[5] were introduced.

The currently popular recipe for monolayer graphene growth was first introduced by Li *et al.*[6] and employs a low-pressure mixture of methane and hydrogen flowing over Cu substrate heated to a temperature slightly below its melting point (~1000 °C).[7] Because of a low solubility of carbon in Cu, the growth is restrained to the surface of the catalyst, thus allowing formation of single layer graphene.[8] Detailed analyses revealed that such samples are typically made of randomly oriented domains[9] in which scattering at the boundaries leads to lower charge carrier mobilities as compared to exfoliated single domain samples. The latest improvements of this protocol allowed higher regions of single domains (up to 0.5 mm was reported)[10] and carrier mobilities, 4000 $cm^2/(V\ s)$, close to those in exfoliated samples.[11]

Despite these improvements, many details in the protocol remain unclear and require thorough examination for ultimate control of the graphene quality. One of the mysterious components is hydrogen, the concentration of which is varied in published recipes with values from zero[12] to thousands times the amount of methane.[13] To clarify this issue and identify routes to grow large size single domain graphene monolayers, we focus on the ambient pressure protocol for growth on Cu foil with Ar as a buffer gas and very low partial pressure of methane (30 ppm) allowing monitoring individual graphene domains as a function of hydrogen pressure. We chose ambient pressure conditions as technologically more attractive in desired production of continuous graphene. However, similar growth results were observed at low pressure CVD as well.

As it follows, graphene growth is strongly dependent on the hydrogen contribution, which seems to serve a double role as an activator of surface-bound carbon that leads to monolayer growth and as an etching reagent that controls the size and morphology of the resulting graphene domains. As a consequence, the growth rate has a maximum as a function of hydrogen partial pressure. The morphology and size of these domains change along with that pressure. No graphene growth is observed

* Address correspondence to vlassioukiv@ornl.gov, snsm@nmsu.edu.

Received for review May 29, 2011 and accepted June 27, 2011.

Published online June 27, 2011
10.1021/nn201978y

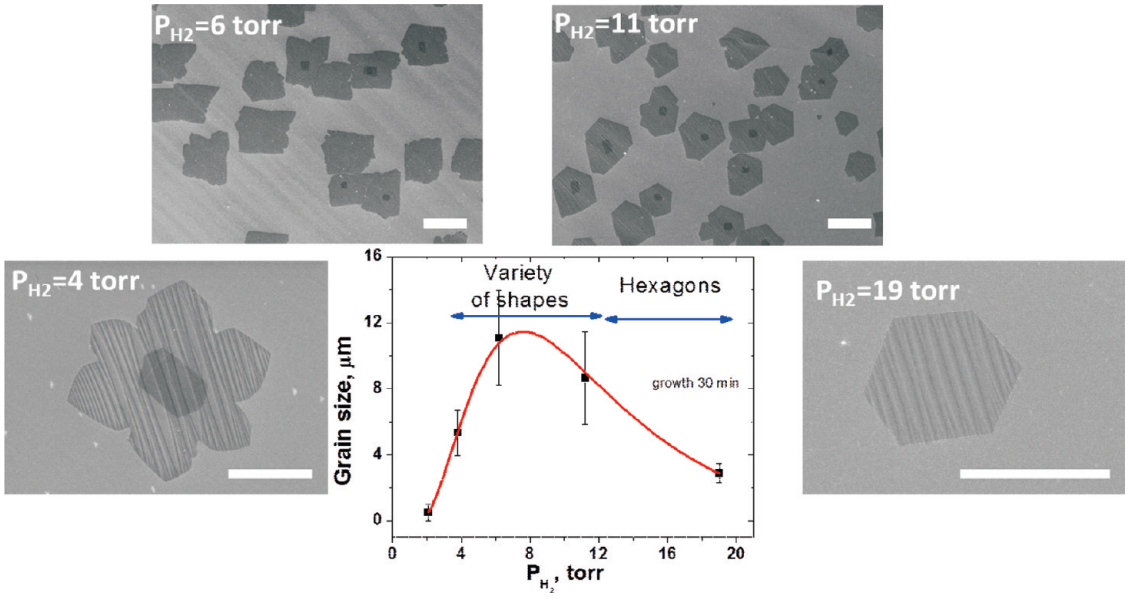

Figure 1. The average size of graphene grains grown for 30 min at 1000 °C on Cu foil using 30 ppm methane in Ar mixture at 1 atm, as a function of partial pressure of hydrogen. The inserts illustrate SEM images of the typical shapes under these different conditions. Note that perfect hexagons are observed only at higher hydrogen pressures. Irregularly shaped grains grown at low hydrogen pressure have smaller size second layers (and even third layers on some) in the centers of grains. Scales bars are 10 μm (top two images) and 3 μm (bottom two images).

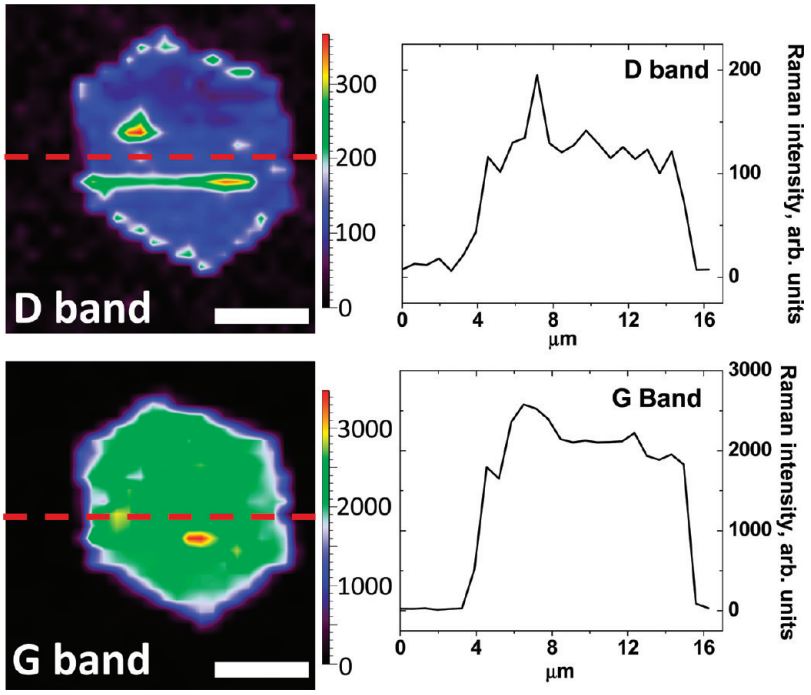

Figure 2. Maps of a hexagonal grain, grown for 90 min on Cu foil using 30 ppm of methane and 19 Torr of hydrogen, and transferred onto SiO_2 (300 nm on Si) using Raman D band (top) and G band (bottom). Note that the D band intensity is low at the edges, as well as in the middle, of the grain. Scale bar is 5 μm.

at very low hydrogen pressures (but sufficient enough to ensure reduction of any oxygen impurities). At intermediate pressures, near maximal rates of growth, the shapes are not regular with some propensity of 6-fold domains with mostly irregular edges, but sometimes 60° edges can be identified. Nearly perfect hexagons are observed at high hydrogen pressures (>10 Torr for 30 ppm of CH_4), and their growth ceases at a size which is dependent on the hydrogen pressure. The Raman analysis suggests that the edges are of zigzag symmetry in agreement with the structure's greater stability.

RESULTS AND DISCUSSION

The conditions used in this study are chosen to elucidate the mechanism of single domain growth. A very low partial pressure of methane (~30 ppm or 23 mTorr) in an atmospheric pressure flow of Ar allows the monitoring of nonoverlapping domains in most cases under study.

The solubility of carbon in Cu is very low, which makes it different from other catalytic metal surfaces as preferentially producing single (occasionally double and triple) layer graphitic structures. Chemisorption of methane on Cu with formation of $(CH_{x<4})_s$ surface-bound active carbon is thermodynamically unfavorable, but if formed, $(CH_x)_s$ agglomeration into multimeric $(C_nH_y)_s$ species is a thermodynamically favorable process ultimately leading to growth of graphitic carbon.[14] It has been shown that formation of CH_x in the gas phase is even less feasible, and when the Cu surface is already covered with carbon, the next layer graphene growth is extremely slow.[15] Because of that and a low concentration of methane in the feed, no growth of graphene is observed in our experiments by SEM without additional cocatalyst, that is, hydrogen (Figure 1). To some extent, hydrogen also counteracts the detrimental effects of stray oxygen and/or other oxidizing contaminants that might be present in the feed and on the copper foil but we observe no growth of graphene on clean "high purity" Cu for partial pressures below 2 Torr (for 30 ppm of CH_4) despite the use of highest purity Ar, CH_4, and H_2 and exhaustive controls for possible contaminants. Increasing the partial pressure of hydrogen, $P_{H_2} > 2$ Torr, was necessary to observe any growth of graphene. As Figure 1 illustrates, the shapes and sizes of graphene grains dramatically change with different pressures of hydrogen. The samples grown at low hydrogen pressures show relatively irregular shaped grains, typically with a second layer (and often with a third) of smaller areas in the grains' centers. The high hydrogen pressure samples, on the other hand, show very regular hexagons with well-identifiable 120° corners. The Raman map of hexagonal grains transferred onto SiO_2 shows very small intensity of the D band throughout the hexagonal grain and even at the edges suggesting the zigzag termination, as Figure 2 demonstrates. It has been previously confirmed that the armchair edges have distinctly higher D band intensity than the zigzag edges because of a lower symmetry of the former.[16] Even though the grains grown at low hydrogen pressures sometime exhibit lobes with 6-fold symmetry, their edges are poorly defined, hence suggesting a mixture of zigzag and armchair termination. Nevertheless, the quality of graphene within the irregularly shaped grains remains similarly high as they also show low D band intensities.[6]

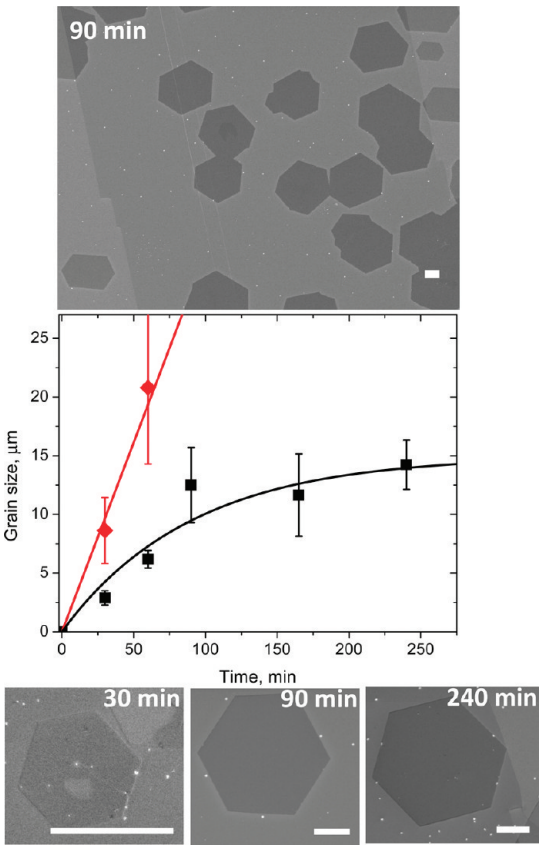

Figure 3. The average size of graphene grains as a function of growth time at 1000 °C on Cu foil using 30 ppm methane in Ar mixture at 1 atm with 19 Torr H_2 (black squares) and with 11 Torr H_2 (red diamonds). SEM images show hexagon size evolution during growth using 19 Torr of H_2. Scale bars are 3 μm.

The graphene growth kinetics for the two representative partial pressures of hydrogen are given in Figure 3. The lower pressure (11 Torr) one, corresponding to the near maximum growth rate in Figure 1, has fewer points and large error bars because of higher surface coverage by graphene for these samples; intergrain separation restricts the maximum grain size. The higher hydrogen pressure (19 Torr in Figure 3) kinetics, on the other hand, clearly demonstrates a saturation behavior, where hexagonally shaped graphene grains cease to grow beyond ~12 μm (edge-to-edge). Unfortunately, it is difficult to control the density of nucleation seeds for graphene growth, and thus we cannot verify whether the low hydrogen pressure kinetics saturates at a higher grains size but it is clear that the regular hexagonal shape is observed only under high enough hydrogen pressure at least under our growth conditions.

This peculiar behavior at different hydrogen pressures is obviously an illustration of the complex role hydrogen plays during this process, at least when methane is used as a carbon source. Without the presence of hydrogen gas in the reaction mixture, methane has to chemisorb on the copper surface to

Scheme 1

$$Cu + H_2 \Leftrightarrow 2H_s \quad (1)$$

$$Cu + CH_4 \rightarrow (CH_3)_s + H_s \text{ - slow} \quad (2)$$

$$Cu + CH_4 \Leftrightarrow (CH_4)_s \quad (3)$$

$$(CH_4)_s + H_s \Leftrightarrow (CH_3)_s + H_2 \quad (4)$$

$$(CH_3)_s + \text{graphene} \Leftrightarrow (\text{graphene+C}) + H_2 \quad (5)$$

$$H_s + \text{graphene} \Leftrightarrow (\text{graphene-C}) + (CH_x)_s \quad (6)$$

form active carbon species, that is, $(CH_3)_s$, $(CH_2)_s$, $(CH)_s$, or C_s, which subsequently react to produce graphene. As shown by experiments and DFT calculations, such dehydrogenation reactions are not thermodynamically favorable even on Cu substrate.[14,17] For example, the first step of methane dehydrogenation with formation of chemisorbed $(CH_3)_s$ radical (reaction 2 in Scheme 1) should overcome a 1.6 eV (~16 kT at 1000 °C) activation barrier with the products being almost 1 eV above the reactants.[14] This endothermic reaction at low methane concentrations should constitute the rate limiting step hindering graphene growth without additional catalysts such as hydrogen. Alternatively, the unfavorable thermodynamics of $(CH_x)_s$ formation might be counteracted by excessive supply of methane allowing for graphene formation without hydrogen[12] but in that route elimination of the second layer growth seems to be problematic. The catalytic role of hydrogen in activating carbon is illustrated by reactions 1 and 4 in Scheme 1. Molecular hydrogen more readily dissociates on copper and forms active hydrogen atoms (1).[18,19] These hydrogen atoms can promote activation of physisorbed methane, which is speculatively described by reaction 4, and lead to formation of surface bound $(CH_3)_s$ radical. Subsequent dehydrogenation steps leading to formation of more active surface bound $(CH_2)_s$ and $(CH)_s$ species are even more endothermic, but their role in graphene growth can be even more important.

At this point, we do not intend to discriminate between $(CH_x)_s$ species because they all are unstable toward dimerization and further converging into larger carboneous species eventually leads to the most stable graphene (5). For example, C_5H_x is thought to play an important role in graphene growth on Ru metal.[20] Currently there is no data for examining the initial stages of active carbon nucleation into larger species and eventually graphene, assessing a critical size of graphene at which its movement along the surface ceases and the growth proceeds by assembling smaller species of active carbon onto graphene nuclei. Nevertheless, we see that nucleation occurs on irregularities such as grooves on metal foils and surface contaminations (see Supporting Information). Such contaminants may also arise from the foil, as we see that the density of graphene grains is greater on the "low purity" Cu than on the "high purity" one. Since the density of

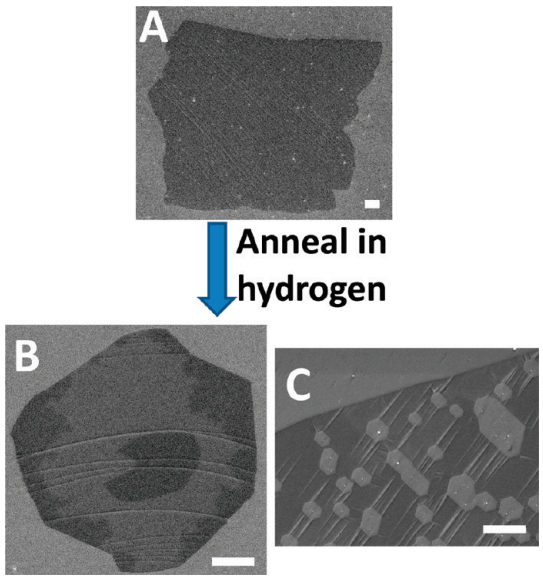

Figure 4. The effect of annealing in hydrogen (19 Torr in 1 atm of Ar, 1000 °C) for graphene grown at low hydrogen pressure: (A) a grain of graphene grown at P_{H_2} = 6 Torr; (B) annealing for 30 min right after deposition demonstrates appearance of 120° angles on the etched edges; (C) annealing after taking the sample to ambient atmosphere deposits dust particles (white spots) that serve as catalytic centers for etching graphene in the middle. Note perfect hexagons with parallel edges in such etched voids. Scale bars are 1 μm.

graphene grains and the total coverage near contamination sites is greater than on cleaner areas, desorption/etching of small active carboneous species is an important part of the overall graphene growth process. Because smaller graphene grains have a higher perimeter to area ratio, they are more vulnerable toward edge etching and, since graphene grain size saturates at high hydrogen partial pressures, hydrogen likely acts not only as a catalyst for carbon activation by dehydrogenation of methane but also participates in controlling the graphene size as depicted in equation 6. It is known that hydrogen can etch carbonaceous materials,[17] and it seems reasonable to assume that it serves a similar role for controlling graphene growth on Cu. The ultimate grain size at high hydrogen pressure corresponds to equilibrium between graphene growth and etching. The hexagonal shape of graphene under the high hydrogen condition suggests a preference for only one type of grain termination, zigzag, as Raman mapping indicates. More importantly, the hexagonal shape of graphene domains unambiguously indicates that the grains are single domains without a need for more elaborate analysis. Hexagonal grains were noticed before, but no explanations were given about underlying causes of their appearance.[21]

The etching effect of hydrogen can proceed not only during growth but also during sample cooling after deposition, which is probably a reason for some researchers' pointing to the need of fast cooling. We have

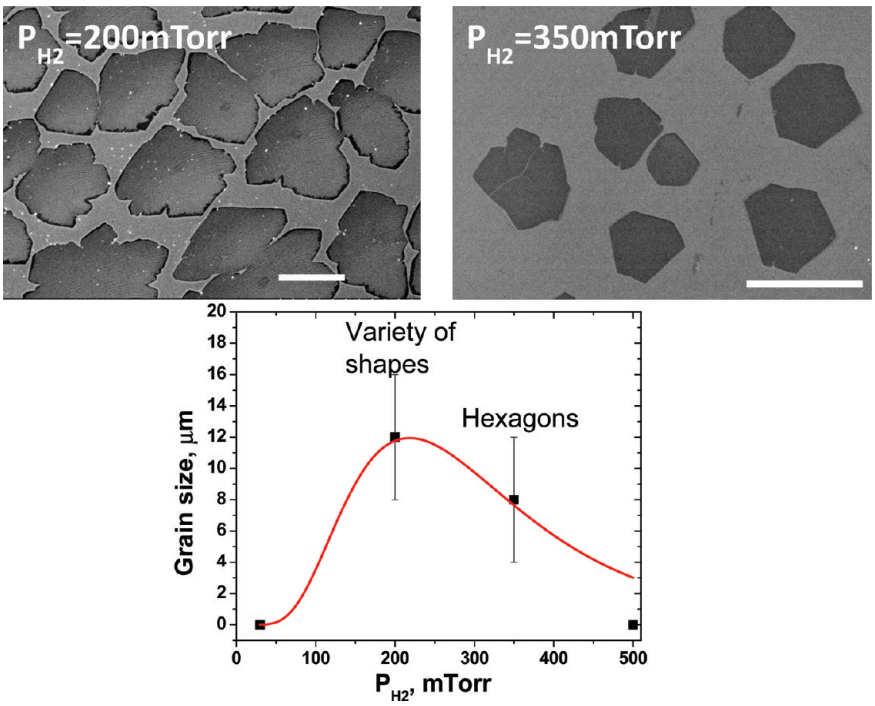

Figure 5. Graphene grains synthesized during 30 min in low-pressure CVD at 1000 °C on Cu foil using 1 mTorr of methane and different partial pressures of hydrogen. Similar to Figure 1 the average size of graphene grains is shown as a function of partial pressure of hydrogen. The inserts illustrate SEM images of the typical shapes; note that hexagons are observed only at high hydrogen pressures. Scale bars are 10 μm.

verified that the minimum temperature at which such etching noticeably occurs for graphene on Cu is no less than 850 °C and thus have focused on annealing at 1000 °C. Graphene grown at low hydrogen pressure has irregularly shaped grains but their annealing at 19 Torr of H_2 for 30 min produces clearly identifiable 120° edges on a large portion of grains (see Figure 4B). If the annealing is performed after the sample is taken out, some dust particles uncontrollably deposited on the surface become the activation centers of graphene etching. Such particles were observed in variable quantities on many samples despite our best efforts in cleaning the tube reactor and controlling the samples environmental exposure available to us outside the clean room. Figure 4C illustrates that etching around these particles, appearing as white dots in SEM, proceeds with formation of holes in graphene having perfect hexagonal shape. Moreover, all these holes have edges parallel to the outside edges. We could not totally avoid these particles in the samples that were taken out of the growing chamber nor could we identify their nature. The appearance of oxygen in EDX spectra suggests the likely presence of some oxides. Note that no etching occurs in the middle of graphene without such particles, corroborating that hydrogen activation occurs on the Cu surface. According to Krauss *et al.*,[22] molecular oxygen etches zigzag and armchair edges equally well and produces circular holes in graphene, in drastic contrast to hexagonal holes observed during slow etching by silicon oxide surface and for etching around nanoparticles reported here.

A similar dependence on hydrogen pressure is also observed with other buffer gases and in low-pressure CVD (see Figure 5). Replacement of Ar for much lighter He in ambient-pressure CVD makes no difference for the same concentrations of hydrogen and methane (see Supporting Information) despite a three times greater collision frequency of buffer molecules with the surface. Under low-pressure CVD conditions, where no buffer gas is present, the maximum growth rate is observed for a very similar ratio of gases' partial pressures, $P_{H_2}/P_{CH_4} \approx 200-300$, despite more than an order of magnitude difference in the actual pressures, 23 mTorr (30 ppm) for APCVD and 1 mTorr for LPCVD. It suggests that formation and etching reactions of graphene have the same order by concentrations of methane and hydrogen, most likely the first order. We have not investigated the regime of extremely elevated methane concentrations (with zero hydrogen pressures),[12] which employs a different mechanism of carbon activation and cannot predict its performance but suspect it would be more difficult in controlling the bilayer formation. At least, we see a larger contribution of bilayers and multilayers in the protocol with hydrogen cocatalyst when methane partial pressure is increased. One can notice different graphene morphologies near the maximum growth rate in Figures 1 and 5. While the latter shows irregular single layer grains, the former has a significant portion of multilayers.

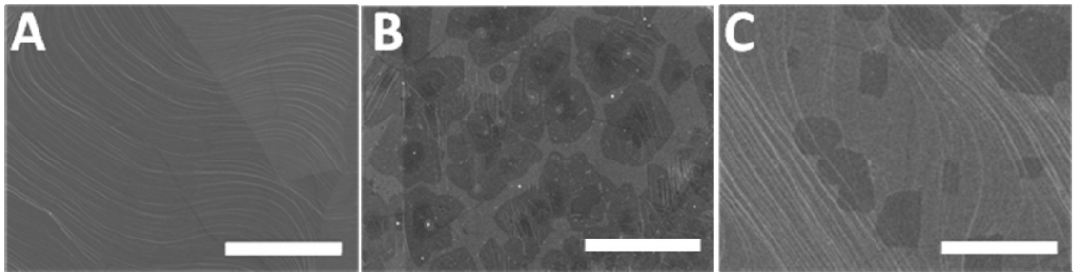

Figure 6. Influence of methane concentration on graphene growth. (A) Continuous single layer is observed at low methane concentration, 30 ppm, grown for 8 h. (B) Second (and sometimes third and fourth) layer appears at a higher methane concentration, 150 ppm, (grown for 30 min) but only at smaller areas in the middle. Note a difference with distinct hexagons of multilayered graphene grown at intermediate methane concentrations (Figure 7). (C) Stepwise increase of methane concentration from 30 to 150 ppm for total of 2.5 h (30 ppm for 90 min, 45 ppm for 15 min, 60 ppm for 15 min, 120 ppm for 15 min, and 150 ppm for 15 min) produces primarily single layer grains with almost no bilayers. The hydrogen partial pressure was 19 Torr in all cases. Scale bars are 10 μm.

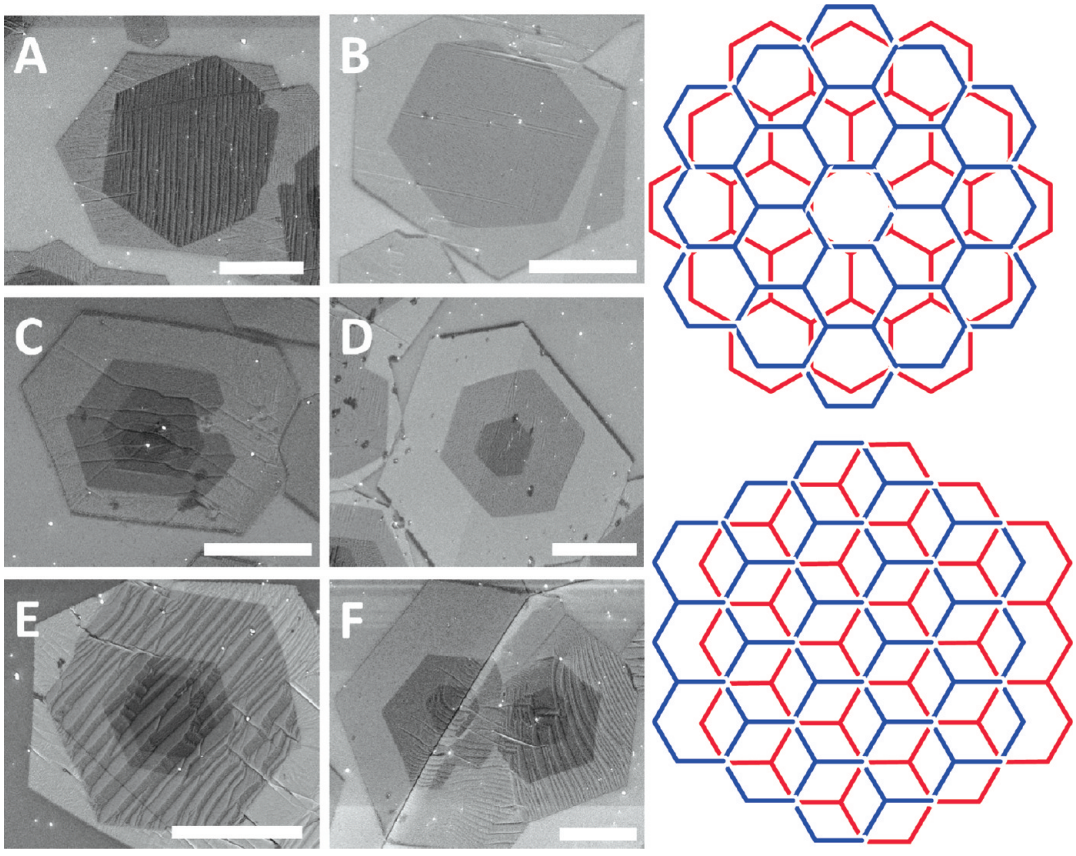

Figure 7. Analysis of mutual orientation between the layers in multilayered graphene grown for 30 min at 60 ppm CH_4, 19 Torr hydrogen pressure. All layers have hexagonal shapes in distinct contrast to irregular grains at higher methane concentrations shown in Figure 6B. The second layer often appears misoriented with respect to the first layer, frequently showing 30 degree rotation (right graphic) (A,B,E), while some do show what resembles AB Bernal stacking (C,D). The third and fourth layers, on the other hand, always show AB stacking (C–F). Scale bars are 3 μm.

This illustrates a limitation of analysis based solely on the P_{H_2}/P_{CH_4} ratio—increasing of methane partial pressure leads to multilayers, as will be discussed below. One should note that the second and higher layers are never complete.

Even though individual graphene grains saturate in size at high hydrogen pressure in Figure 1, their density eventually increases enough to connect the grains and cover the whole surface, as shown in Figure 6A. Note that the coverage corresponds to a perfect single layer but not to a single domain as the original domains' orientations were random (Supporting Information). This total coverage is achieved at relatively long growth times. The rate of growth can be accelerated by increasing the methane concentration but it also promotes growth of the second layer (and even greater

multilayers), as shown in Figure 6B for 150 ppm of methane. At this high methane pressure, the second and third graphene layer grains' shapes appear irregular but at intermediate pressures, for example, 60 ppm in Figure 7, all layers are almost hexagonal in shape. This observation suggests that hydrogen etches not only the first layer but the top layers as well. The rate of grain growth at a high methane supply overcomes the etching effect by hydrogen resulting in irregular shapes of graphene grains (Figure 6B). Note that the relative orientation of the first two layers does not always correspond to AB Bernal staking (Figure 7C, D); some of them frequently show rotation close to 30° (Figure 7 A,B,E). The behavior is puzzling, but can be related to the fact that orientation of the second layer is not solely determined by interaction with the first graphene layer—copper catalyst also participates in defining the orientation, despite the separation due to the first layer. The third and fourth layers, on the other hand, almost exclusively show commensurate AB stacking with the second layer suggesting that interaction with copper is negligible for the third layer and above. Since these additional top layers appear in the middle of the graphene grain,[23] their formation likely occurs only at the beginning when the amount of supplied active surface-bound carbon exceeds what can be consumed by small perimeter of a graphene grain. Upon reaching a large enough size, the amount of produced active carbon decreases due to a smaller area of open Cu, and it is mostly consumed by the first layer graphene. To corroborate that, we have gradually increased the concentration of methane from 30 ppm to 150 ppm while maintaining the same amount of hydrogen. As Figure 6C shows, most of the copper area is covered by the single layer graphene grains with small densities of bilayers (darker regions), in drastic contrast to using 150 ppm of methane from the beginning, when a significant portion of grains is multilayered (Figure 6B).

Thus, to grow a single layer single domain graphene on Cu, it is important to ensure the presence of single seed and control the supply of methane with excess of hydrogen (approximately by a factor 300 at 1000 °C) in the beginning and gradually increase the supply of methane. Such growth regime can be achieved in both, ambient pressure and low pressure CVD conditions. The most challenging part we could not realize yet is the desired single seed requirement, without which high quality single layer graphene still grows but not as a single domain.

CONCLUSIONS

Thus we have shown that hydrogen plays a dual role in the process of graphene growth by CVD on copper foil with methane as a carbon source. It acts as a cocatalyst in formation of active surface bound carbon species $(C_yH_x)_s$ required for graphene growth and controls the grains shape and dimension by etching away the "weak" carbon−carbon bonds. Graphene nucleation, the growth rate, and the termination size of grains are affected by competition of these two processes. No graphene growth was observed at low partial hydrogen pressures (<2 Torr with 30 ppm of CH_4 and Ar buffer at ambient pressure, that is, $P_{H_2}/P_{CH_4} < 20$) on clean surfaces due to the rate limiting step of methane activation (2), which is thermodynamically unfavorable. At higher hydrogen pressures, hydrogen atoms produced on the copper surface assist in generation of active carbon species (4) required for graphene growth (5). At intermediate hydrogen partial pressures ($P = 2-11$ Torr, that is, $P_{H_2}/P_{CH_4} = 200-400$), graphene grains show a variety of shapes without any recognized preference toward either zigzag or armchair termination. Higher hydrogen pressures ($P \approx 19$ Torr, that is, $P_{H_2}/P_{CH_4} > 400$) result in distinct hexagonal shape of grains and saturation of their size due to etching of the graphene by hydrogen (6). Raman intensity mapping suggests preferential zigzag terminations of such hexagons in line with their predicted lower energy. Elevated methane concentrations tend to promote formation of multilayers; the shape of grains for which are similarly dependent on hydrogen but their coverage is always less than 100%. Hexagonal multilayers have commensurate AB Bernal stacking between the second and higher layers but the mutual orientation of the first two layers is random.

METHODS

Two types of copper foil substrates with different purity, "low" (Alfa Aesar, #13382, 99.8%) and "high" (Alfa Aesar, No. 10950, 99.999%), were employed in CVD synthesis of graphene. Similar results were obtained on both but with a greater density (Supporting Information) of individual grains on the "low" quality foils. Before CVD, foils were cleaned by acetone, isopropyl alcohol (IPA), deionized (DI) water, and IPA again. Additional cleaning by diluted (1%) HNO_3 did not produce any changes in graphene grain appearance. CVD growth under ambient pressure was performed in a 3″ quartz tube with the total gas flow of 500 sccm (cm^3 per min). The desired partial pressures of H_2 and CH_4 were achieved by mixing the stock gas mixtures of 2.5% H_2 and 0.1% CH_4 in Ar with high purity argon. The foils were heated to 1000 °C in the hydrogen stock mixture (2.5% H_2 in Ar) with the rate of 10 °C/min and annealed for 1 h with the subsequent graphene growth at 1000 °C upon adding argon and the stock methane mixture to a desired proportion for a chosen time. Samples were fast cooled to room temperature in the same mixture but without methane flow. Further analyses were performed typically within a few days. For LPCVD growth, the pressure was lowered below 500 mTorr. Methane

partial pressure was kept at 1 mTorr, and the hydrogen partial pressure was systematically varied.

For Raman characterization, graphene was transferred onto 300 nm SiO_2/Si wafer using spin-coated PMMA (~500 nm thick) with its subsequent dissolution in acetone.[6] Raman spectra were obtained with 633 nm laser excitation using Renishaw confocal instrument.

Acknowledgment. I.V. is a Eugene P. Wigner Fellow at the Oak Ridge National Laboratory, managed by UT-Battelle, LLC, for the U.S. Department of Energy under Contract DE-AC05-00OR22725. A portion of this research was conducted at the Center for Nanophase Materials Sciences, which is sponsored at Oak Ridge National Laboratory by the Scientific User Facilities Division, U.S. Department of Energy. The LPCVD part of the work was supported by the Materials Science and Engineering Division through Basic Energy Sciences Program. P.F.F. and S.D. were supported as part of the Fluid Interface Reactions, Structures and Transport (FIRST) Center, an Energy Frontier Research Center funded by the US Department of Energy, Office of Science, Office of Basic Energy Sciences under Award No. ERKCC61

Supporting Information Available: SEM images illustrating (a) mutual orientation of graphene grains; (b) the effect of copper purity and surface morphology on the graphene nucleation density; (c) the effect of the buffer gas; (d) additional images illustrating the effect of hydrogen partial pressure and the methane partial pressure on the shape and morphology of graphene grains; Raman spectra for monolayers grown at the conditions for hexagonal and irregularly shaped graphene grains. This material is available free of charge *via* the Internet at http://pubs.acs.org.

REFERENCES AND NOTES

1. Novoselov, K. S.; Geim, A. K.; Morozov, S. V.; Jiang, D.; Zhang, Y.; Dubonos, S. V.; Grigorieva, I. V.; Firsov, A. A. Electric Field Effect in Atomically Thin Carbon Films. *Science* **2004**, *306*, 666–669.
2. Geim, A. K.; Novoselov, K. S. The Rise of Graphene. *Nat. Mater.* **2007**, *6*, 183–197.
3. Geim, A. K. Graphene: Status and Prospects. *Science* **2009**, *324*, 1530–1534.
4. Bae, S.; Kim, H.; Lee, Y.; Xu, X.; Park, J.-S.; Zheng, Y.; Balakrishnan, J.; Lei, T.; Kim, H. R.; Song, Y.; *et al.* Roll-to-Roll Production of 30-in. Graphene Films for Transparent Electrodes. *Nat. Nanotechnol.* **2010**, *5*, 574.
5. Zhu, Y.; Murali, S.; Cai, W.; Li, X.; Suk, J. W.; Potts, J. P.; Ruoff, R. S. Graphene and Graphene Oxide: Synthesis, Properties and Applications. *Adv. Mater.* **2010**, *22*, 3906–3924.
6. Li, X.; Cai, W.; An, J.; Kim, S.; Nah, J.; Yang, D.; Piner, R.; Velamakanni, A.; Jung, I.; Tutuc, E.; *et al.* Large-Area Synthesis of High-Quality and Uniform Graphene Films on Copper Foils. *Science* **2009**, *324*, 1312–1314.
7. Vlassiouk, I.; Smirnov, S.; Ivanov, I.; Fulvio, P.; Dai, S.; Meyer, H.; Chi, M.; Hensley, D.; Datskos, P.; Lavrik, N. Electrical and Thermal Conductivity of Low Temperature CVD Graphene: the Effect of Disorder. *Nanotechnology* **2011**, *22*, 275716.
8. Li, X.; Cai, W.; Colombo, L.; Ruoff, R. S. Evolution of Graphene Growth on Ni and Cu by Carbon Isotope Labeling. *Nano Lett.* **2009**, *9*, 4268.
9. Huang, P. Y.; Ruiz-Vargas, C. S.; van der Zande, A. M.; Whitney, W. S.; Levendorf, M.; Kevek, J.; Garg, S.; Alden, J. S.; Hustedt, C. J.; Zhu, Y.; *et al.* Grains and Grain Boundaries in Single-Layer Graphene Atomic Patchwork Quilts. *Nature* **2011**, *469*, 389.
10. Li, X.; Magnuson, C. W.; Venugopal, A.; Tromp, R. M.; Hannon, J. B.; Vogel, E. M.; Colombo, L.; Ruoff, R. S. Large-Area Graphene Single Crystals Grown by Low-Pressure Chemical Vapor Deposition of Methane on Copper. *J. Am. Chem. Soc.* **2011**, *133*, 2816.
11. Li, X.; Magnuson, C. W.; Venugopal, A.; An, J.; Suk, J. W.; Han, B.; Borysiak, M.; Cai, W.; Velamakanni, A.; Zhu, Y.; *et al.* Graphene Films with Large Domain Size by a Two-Step Chemical Vapor Deposition Process. *Nano Lett.* **2010**, *10*, 4328–4334.
12. Gao, L.; Ren, W.; Zhao, J.; Ma, L.-P.; Chen, Z; Cheng, H.-M. Efficient Growth of High-quality Graphene Films on Cu Foils by Ambient Pressure Chemical Vapor Deposition. *Appl. Phys. Lett.* **2010**, *97*, 183109.
13. Bhaviripudi, S.; Jia, X.; Dresselhaus, M.; Kong, J. Role of Kinetic Factors in Chemical Vapor Deposition Synthesis of Uniform Large Area Graphene Using Copper Catalyst. *Nano Lett.* **2010**, *10*, 4128.
14. Zhang, W.;Wu, P.; Li, Z.; Yang, J. First-Principles Thermodynamics of Graphene Growth on Cu Surface. arXiv: 1101.3851v1
15. Alstrup, I.; Chorkendorff, I.; Ullman, S. The Interaction of CH_4 at High Temperatures with Clean and Oxygen Precovered Cu(100). *Surf. Sci.* **1992**, *264*, 95–102.
16. Chae, D.-H.; Krauss, B.; von Klitzing, K.; Smet, J. H. Hot Phonons in an Electrically Biased Graphene Constriction. *Nano Lett.* **2010**, *10*, 466–471.
17. Galea, N. M.; Knapp, D.; Ziegler, T. Density Functional Theory Studies of Methane Dissociation on Anode Catalysts in Solid-Oxide Fuel Cells: Suggestions for Coke Reduction. *J. Catal.* **2007**, *247*, 20.
18. Gelb, A.; Cardillo, M. Classical Trajectory Studies of Hydrogen Dissociation on a Cu(100) Surface. *Surf. Sci.* **1976**, *59*, 128 and references therein.
19. Gelb, A.; Cardillo, M. Classical Trajectory Study of the Dissociation of Hydrogen on Copper Single Crystals. II. Cu(100) and Cu(110). *Surf. Sci.* **1977**, *64*, 197 and references therein.
20. Zangwill, A.; Vvedensky, D. Novel Growth Mechanism of Epitaxial Graphene on Metals. *Nano Lett.* **2011**, *11*, 2092–2095.
21. Yu, Q.; Jaurengui, L. A.; Wu, W.; Colby, R.; Tian, J.; Su, Z.; Cao, H.; Liu, Z.; Pandey, D.; Wei, D.; *et al.* Control and Characterization of Individual Grains and Grain Boundaries in Graphene Grown by Chemical Vapor Deposition. *Nat. Mater.* **2011**, *10*, 443–449.
22. Krauss, B.; Nemes-Incze, P.; Skakalova, V.; Biro, P.; Klitzing, K.; Smet, J. Raman Scattering at Pure Graphene Zigzag Edges. *Nano Lett.* **2010**, *10*, 4544–4548.
23. Robertson, A; Warner, J. Hexagonal Single Crystal Domains of Few Layer Graphene on Copper Foils. *Nano Lett.* **2011**, *11*, 1182.